COMMUNICATION

A salt-bridge structure in solution revealed by 2D-IR spectroscopy†

Adriana Huerta-Viga, Sérgio R. Domingos, Saeed Amirjalayer and Sander Woutersen*

Salt bridges are important interactions for the stability of protein conformations, but up to now it has been difficult to determine salt-bridge geometries in solution. Here we characterize the spatial structure of a salt bridge between guanidinium (Gdm$^+$) and acetate (Ac$^-$) using two-dimensional vibrational (2D-IR) spectroscopy. We find that as a result of salt bridge formation there is a significant change in the infrared response of Gdm$^+$ and Ac$^-$, and cross peaks between them appear in the 2D-IR spectrum. From the 2D-IR spectrum we determine the relative orientation of the transition-dipole moments of the vibrational modes of Gdm$^+$ and Ac$^-$, as well as the coupling between them.

Salt bridges are hydrogen-bonded ion pairs that are important for the stabilization of molecular conformations. Intermolecular salt bridges are used to create new supramolecular systems,[1,2] while biological systems such as proteins often contain salt bridges that determine their structure[3] and function.[4] To understand the chemical functionality of salt bridges, it is essential to detect salt-bridged ion pairs and to characterize their solvated structure, which is unfortunately difficult with conventional methods such as NMR. Here we report the study of a biologically-relevant ion pair formed by guanidinium (Gdm$^+$) and acetate (Ac$^-$), using two-dimensional infrared (2D-IR) spectroscopy. This technique is used to measure the vibrational coupling between transition-dipole moments of individual vibrations, and through a quantitative analysis of the 2D-IR spectrum, structural information can be obtained.[5,6] The Gdm$^+$···Ac$^-$ ion pair is a model for salt bridges between the Gdm$^+$ side group of arginine and the carboxylate side group of glutamate or aspartate, which occur commonly in proteins.[7] The molecular structure of this ion pair is shown in Fig. 1A. Isolated Gdm$^+$ has D_3 symmetry, and has a degenerate mode due to a combined CN$_3$ antisymmetric stretch and NH$_2$ scissors motion at a frequency of 1600 cm^{-1}.[8] This degeneracy is

observed in aqueous solution, but it is broken in viscous solvents.[9] When dissolving deuterated Gdm$^+$ (guanidine·DCl, >98% purity, 400 mM) in deuterated dimethylsulfoxide (DMSO), we observe a splitting between the frequencies of the two CN$_3$D$_6^+$ modes, as can be seen in Fig. 1B. In the following, we refer to the high- and low-frequency CN$_3$D$_6^+$ modes of Gdm$^+$ as Gdm$_{HF}^+$ and Gdm$_{LF}^+$, respectively. Interestingly, when an equimolar amount of Ac$^-$ ions is added to the solution (guanidine acetate salt, >98% purity, 400 mM), the splitting between Gdm$_{HF}^+$ and Gdm$_{LF}^+$ becomes larger, as seen in Fig. 1B. Gdm$^+$ and Ac$^-$ have a strong binding affinity in DMSO, forming more than 98% dimers at the concentration used in our experiments,[10] which suggests that the larger splitting between the Gdm$^+$ modes is due to an interaction with the Ac$^-$ ion. Moreover, Ac$^-$ (tetrabutylammonium acetate, >97% purity) has an absorption band at 1580 cm^{-1} in DMSO (shown in Fig. 1B) due to the COO$^-$-antisymmetric-stretch mode. This mode red-shifts after dimer formation with Gdm$^+$. The change in the infrared response of both the Gdm$^+$ and the Ac$^-$ ions upon dimer formation strongly suggests that there is a coupling between the vibrational modes of these two molecules.
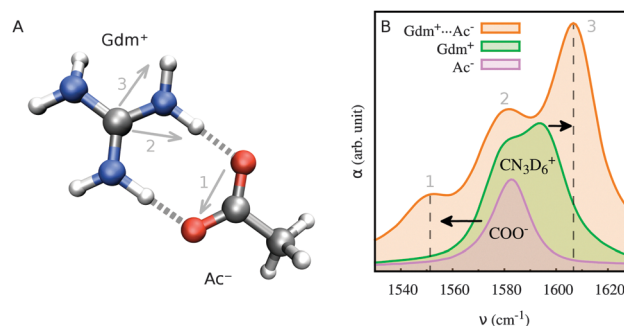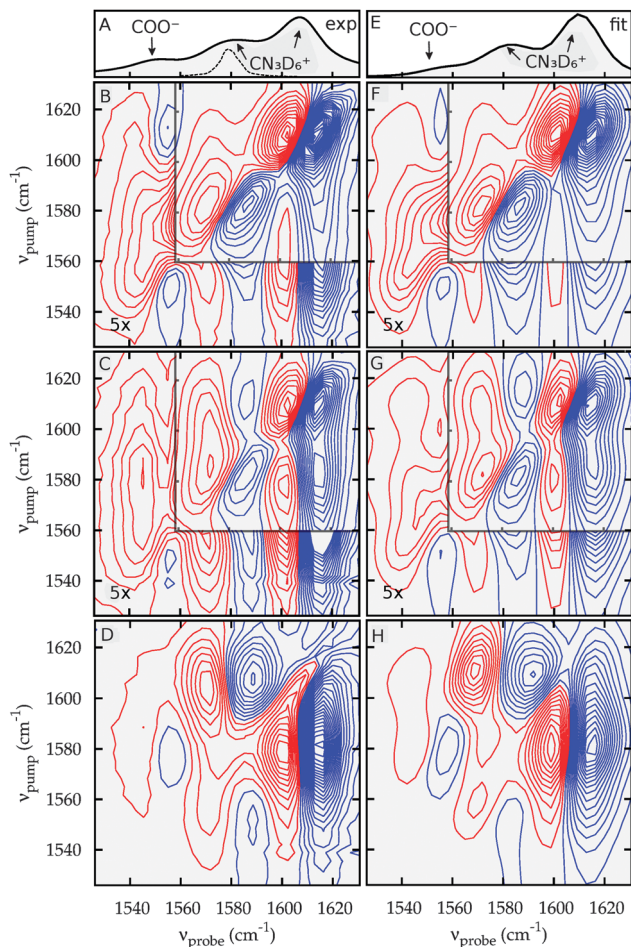

Fig. 1 (A) Molecular structure of the Gdm$^+$···Ac$^-$ dimer obtained using *ab initio* methods. The corresponding transition-dipole moments of the COO$^-$-stretch mode (1) and of the CN$_3$D$_6^+$ low- and high- frequency modes (2 and 3, respectively) are indicated by arrows. (B) Infrared absorption spectrum of Gdm$^+$···Ac$^-$, Gdm$^+$ and Ac$^-$ in DMSO (solvent subtracted). Shifts of the COO$^-$ and high-frequency CN$_3$D$_6^+$ bands are indicated by arrows.

Van't Hoff Institute for Molecular Sciences (HIMS), University of Amsterdam, Science Park 904, Amsterdam, The Netherlands. E-mail: S.Woutersen@uva.nl; Fax: +31 2052 56456; Tel: +31 2052 57091

15784 | *Phys. Chem. Chem. Phys.*, 2014, **16**, 15784–15786

This journal is © the Owner Societies 2014

Fig. 2 (A) Infrared absorption spectrum of $Gdm^+\cdots Ac^-$. The dashed line indicates a representative pump–pulse spectrum. (B) and (C) 2D-IR spectra of $Gdm^+\cdots Ac^-$ for parallel and perpendicular polarization of the pump and probe pulses, respectively (a pump–probe delay of 1.5 ps). Blue indicates negative absorption change, red positive absorption change. The contour intervals are 1 mOD (parallel) and 0.5 mOD (perpendicular), and the left and bottom parts are scaled by a factor of 5, as indicated. (D) Weighted-difference 2D-IR spectrum ($3\Delta\alpha_\perp - \Delta\alpha_\parallel$). The contour intervals are 0.5 mOD. (E) Calculated absorption spectrum with parameters obtained from a fit to the 2D-IR spectrum. (F) and (G) Fitted 2D-IR spectra for parallel and perpendicular polarization of the pump and probe pulses, respectively. The contour intervals are the same as in (B) and (C). (H) Weighted-difference 2D-IR spectrum that was calculated with parameters obtained from a fit to the parallel- and perpendicular-polarization spectra. Contour intervals are the same as in (D).

The 2D-IR spectra of the $Gdm^+\cdots Ac^-$ dimer confirm unambiguously that the Gdm_{HF}^+ and Gdm_{LF}^+ modes are both coupled to the COO^--stretch mode of Ac^-. To measure the 2D-IR spectra, we use a femtosecond pump–probe setup that has been described elsewhere.[11] The 2D-IR spectra are shown in Fig. 2B and C for parallel and perpendicular polarization of the pump and probe pulses, and weighted difference ($3\Delta\alpha_\perp - \Delta\alpha_\parallel$), respectively. The non-zero off-diagonal response (cross peaks) in the 2D-IR spectra indicates that there is a coupling between the two $CN_3D_6^+$ modes of Gdm^+ and, more importantly, between each of them and the COO^--stretch mode of Ac^-. These cross peaks can be seen better in slices along both the pump and probe axes of the 2D-IR spectra. Fig. 3A shows cross sections of
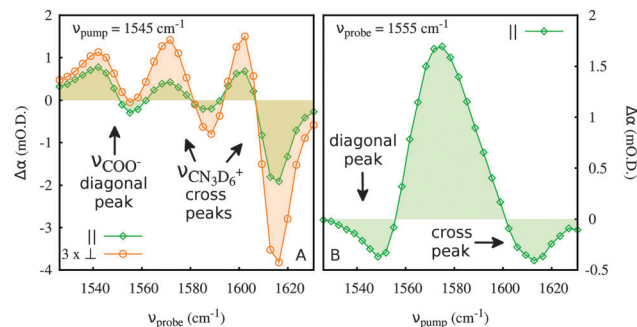
Fig. 3 (A) Cross section along the probe axis of the 2D-IR spectra for parallel and perpendicular polarization of the pump and probe pulses, and for $\nu_{pump} = \nu_{COO^-}$. (B) Cross section along the pump axis of the 2D-IR spectrum for parallel polarization of the pump and probe pulses, and for $\nu_{probe} = \nu_{COO^-}$.

$\nu_{pump} = \nu_{COO^-}$ for parallel and perpendicular polarization of the pump and probe pulses. In the cross sections, the cross peaks between the COO^--stretch mode and each of the Gdm^+ modes are clearly visible. Note that the diagonal signal of the COO^--stretch mode has a smaller magnitude than these cross peaks because of its smaller absorption cross section (see Fig. 1B). Fig. 3B shows a cross section along the probe axis for $\nu_{probe} = \nu_{COO^-}$ for parallel polarization of pump and probe pulses. The negative part at 1550 cm^{-1} is due to the bleaching and $\nu = 1 \rightarrow 0$ stimulated emission of the COO^--stretch mode on the diagonal of the 2D spectrum. The positive region centered at 1580 cm^{-1} is the low-probe-frequency tail of the excited-state absorption of the Gdm_{LF}^+ mode on the diagonal. The negative region at 1610 cm^{-1} is the negative part of the cross peak between the COO^--stretch mode and the Gdm_{HF}^+ mode. Note that the cross peaks between Gdm_{HF}^+ and Ac^- are more clearly visible in the parallel-polarization 2D-IR spectrum (Fig. 2B), and almost vanish in the $3\Delta\alpha_\perp - \Delta\alpha_\parallel$ difference spectrum (Fig. 2D). This behaviour indicates that the transition-dipole moments of these modes are approximately parallel.[12] In contrast, the cross peaks between Gdm_{LF}^+ and Ac^- appear clearly in the $3\Delta\alpha_\perp - \Delta\alpha_\parallel$ difference spectrum (Fig. 2D), which suggests that their transition-dipole moments are at a nonzero angle.[12]

In order to obtain structural information from the 2D-IR spectra, we use a vibrational-exciton model (see ESI† for a description of the model).[12] It has been shown before that in addition to coupling between the two $CN_3D_6^+$ modes, there is also energy transfer between them,[9] but in DMSO this process is slow enough to be neglected at the delay at which we measured the 2D-IR spectra used for the structural analysis (1.5 ps, see ESI†). We determine the spectral and structural parameters from a global fit to the parallel and perpendicular 2D-IR spectra. Fig. 2F and G show the fitted 2D-IR spectra, which are in very good agreement with the measured ones. Note that the difference spectrum, shown in Fig. 2D is not fitted but the corresponding calculated spectrum, shown in Fig. 2H, is also in very good agreement with the measurement. We find that in order to obtain a good fit, an inhomogeneity in the coupling between Gdm_{LF}^+ and Gdm_{HF}^+ modes has to be taken into account in the model.

This journal is © the Owner Societies 2014

Phys. Chem. Chem. Phys., 2014, **16**, 15784–15786 | **15785**

Table 1 Coupling β and angle θ between the transition-dipole moments of the COO$^-$-stretch mode of Ac$^-$ and the two CN$_3$D$_6^+$ modes of Gdm$^+$ as obtained from the fit (χ_r^2 = 41). See ESI for estimates of the confidence limits

Modes	β (cm^{-1})	θ
Gdm$_{HF}^+$–Gdm$_{LF}^+$	−8	105°
Gdm$_{HF}^+$–Ac$^-$	−11	180°
Gdm$_{LF}^+$–Ac$^-$	8	75°

The couplings between the three modes involved in the salt bridge (Gdm$_{HF}^+$, Gdm$_{LF}^+$ and Ac$^-$), and the angles between their transition-dipole moments were parameters of the fit and are listed in Table 1 (see ESI† for a complete list of fit parameters). The coupling between Gdm$_{HF}^+$ and Gdm$_{LF}^+$ modes, which involve oscillations of the same CN and NH bonds, is −8 cm^{-1}. Remarkably, the couplings between the COO$^-$-stretch mode and the Gdm$_{HF, LF}^+$ modes are of a similar magnitude, (−11 and 8 cm^{-1}, respectively) even though these vibrational modes share neither atoms nor bond: these couplings originate purely from the salt bridge between the two molecules. The large couplings between the COO$^-$ and the Gdm$_{HF,LF}^+$ modes show that the frequency shifts observed in the IR spectrum upon salt-bridge formation (Fig. 1A) are mostly due to splitting of the coupled modes rather than due to a change in the local-mode frequencies. This is confirmed by the fact that the COO$^-$ peak shifts much less when acetate forms a salt bridge with protonated Gdm$^+$, in which the two CN$_3$H$_6^+$ modes are at a higher frequency (see ESI†). The angles between the transition-dipole moments of the salt-bridged vibrational modes are in good agreement with the planar geometry shown in Fig. 1A. The planarity of a salt bridge is often taken as a metric of its quality in X-ray studies,[13] and our results suggest that in DMSO solution, the geometry of an isolated salt bridge, in which steric constraints are absent, is indeed planar. This finding is also in agreement with experimental results in peptides in the gas phase, where planar geometries for salt bridges between Arg$^+$ and Glu$^-$ were found.[14,15] We have performed complementary *ab initio* calculations on the Gdm$^+ \cdots$Ac$^-$ dimer using Gaussian03[16] at the MP2/6-311+G(d) level of theory. The calculation predicts a planar geometry for the salt bridge, *i.e.*, the three transition-dipole moments are coplanar, as shown in Fig. 1A. The angle between the transition-dipole vectors of the two Gdm$^+$ modes is smaller than for isolated guanidinium,[9] most likely as a result of salt bridge formation with the Ac$^-$ ion. We find in the calculation that the Gdm$_{HF}^+$ mode is antisymmetric with respect to the symmetry axis through the C–C bond of Ac$^-$, which explains the large coupling with the likewise antisymmetric COO$^-$-stretch mode.[17] The Gdm$_{LF}^+$ mode is symmetric with respect to this symmetry axis, so it is remarkable that it couples quite strongly to the COO$^-$-stretch mode despite their different symmetry. The infrared-absorption bands predicted from the *ab initio* calculations also show a shift of the Gdm$^+$ modes upon salt bridge formation, in agreement with our measurements (see ESI†).

In conclusion, we were able to detect the existence of a salt bridge between Gdm$^+$ and Ac$^-$ in solution using 2D-IR spectroscopy. The method we present is also applicable for the detection of salt bridges between arginine and glutamate or aspartate in peptides and proteins. Spectral crowding due to the broadening of the amide I band in larger systems can be avoided by using isotopic labels: ^{15}N for Arg$^+$ results in $\sim$40 cm^{-1} redshift,[18] and ^{18}O for Glu$^-$ results in $\sim$10 cm^{-1} redshift.[12] We characterize the coupling between two CN$_3$D$_6^+$ modes of Gdm$^+$ and the COO$^-$-stretch mode of Ac$^-$, and we find that the COO$^-$-stretch mode couples more strongly to the high-frequency CN$_3$D$_6^+$ mode than to the low-frequency one, most likely because of their similar symmetry. Our data indicate a salt-bridge geometry in which the Gdm$^+$ and COO$^-$ moieties are coplanar. Our results show that 2D-IR spectroscopy is a method of wide applicability to detect and determine the geometry of salt bridges in solution, with picosecond temporal resolution.

References

1 B. Kuberski and A. Szumna, *Chem. Commun.*, 2009, 1959–1961.
2 L. E. R. O'Leary, J. A. Fallas, E. L. Bakota, M. K. Kang and J. D. Hartgerink, *Nature Chem.*, 2011, **3**, 821–828.
3 S. Kumar and R. Nussinov, *J. Mol. Biol.*, 1999, **293**, 1241–1255.
4 J. M. Christie, A. S. Arvai, K. J. Baxter, M. Heilmann, A. J. Pratt, A. O'Hara, S. M. Kelly, M. Hothorn, B. O. Smith, K. Hitomi, G. I. Jenkins and E. D. Getzoff, *Science*, 2012, **335**, 1492–1496.
5 O. Golonzka and A. Tokmakoff, *J. Chem. Phys.*, 2001, **115**, 297.
6 M. T. Zanni, N. H. Ge, Y. S. Kim and R. M. Hochstrasser, *Proc. Natl. Acad. Sci. U. S. A.*, 2001, **98**, 11265–11270.
7 K. D. Walker, T. P. Causgrove and R. T. Sauer, *J. Mol. Model.*, 2009, **15**, 1213–1219.
8 R. J. Sension and B. Hudson, *J. Phys. Chem.*, 1990, **94**, 4015–4025.
9 D. Y. Vorobyev, C.-H. Kuo, D. G. Kuroda, J. N. Scott, J. M. Vanderkooi and R. M. Hochstrasser, *J. Phys. Chem. B*, 2010, **114**, 2944–2953.
10 B. Linton and A. D. Hamilton, *Tetrahedron*, 1999, **55**, 6027–6038.
11 A. Huerta-Viga, D. J. Shaw and S. Woutersen, *J. Phys. Chem. B*, 2010, **114**, 15212–15220.
12 P. Hamm and M. Zanni, *Concepts and Methods of 2D Infrared Spectroscopy*, Cambridge University Press, 1st edn, 2011.
13 J. E. Donald, D. W. Kulp and W. F. DeGrado, *Proteins*, 2011, **79**, 898–915.
14 A. M. Rijs, G. Ohanessian, J. Oomens, G. Meijer, G. von Helden and I. Compagnon, *Angew. Chem., Int. Ed.*, 2010, **49**, 2332–2335.
15 S. Jaeqx, J. Oomens and A. M. Rijs, *Phys. Chem. Chem. Phys.*, 2013, **15**, 16341–16352.
16 M. J. Frisch, *et al.*, *Gaussian 03, Revision C.02*, Gaussian, Inc., Wallingford, CT, 2004.
17 B. Sharma, *Spectroscopy*, Krishna Prakashan, 1981.
18 I. T. Arkin, *Curr. Opin. Chem. Biol.*, 2006, **10**, 394–401.

15786 | *Phys. Chem. Chem. Phys.*, 2014, **16**, 15784–15786

This journal is © the Owner Societies 2014